# Journal of Materials Chemistry C

Accepted Manuscript


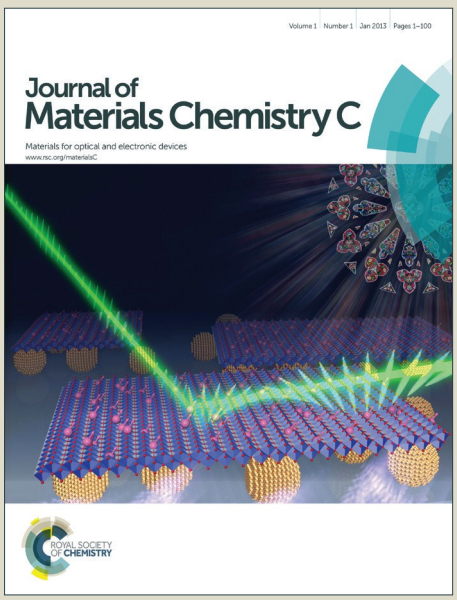





ROYAL SOCIETY OF CHEMISTRY

www.rsc.org/materialsC

Journal of Materials Chemistry C

PAPER

# Large-area, stretchable, super flexible and mechanically-stable thermoelectric films of polymer/carbon nanotube composites

Received 00th January 20xx,
Accepted 00th January 20xx

DOI: 10.1039/x0xx00000x

www.rsc.org/

Lirong Liang,[abc] Caiyan Gao,[a] Guangming Chen*[a] and Cun-Yue Guo*[b]

Recently, due to their unique advantages over inorganic materials, organic polymer thermoelectric (TE) materials have received considerable attention. However, most studies focus on TE performance enhancement. So far, little attention has been paid to large-area preparation, stretchability, super flexibility and mechanical stability, although they are the intrinsic advantages of polymer materials. Here we report for the first time large-area, stretchable, super flexible and mechanically-stable TE films of polymer/carbon nanotube composites. Mechanically stretchable films with diameter of ~18 cm are achieved by common vacuum filtration, whose thicknesses and sizes can be conveniently adjusted. Despite direct observations of films under various deformations of bending, rolling or twisting, quantitative measurements of minimum bending radii (< 0.6 mm) further confirm the super flexibility. More importantly, after mechanical bending or stretching, no obvious deterioration of TE performance is found. Our findings represent a novel direction of polymer TE materials, and will speed up their applications.

## Introduction

Thermoelectric (TE) materials, which can realize direct energy conversion between heat and electricity without moving parts and any toxic liquid medium, have widely applications in both TE generators for waste or low-quality heat harvesting and local cooling.[1-3] In the recent few years, organic TE materials, mainly conducting polymers[4-10] and their nanocomposites,[11-17] have sparked intense interest and gained remarkable achievements. For example, addition of carbon nanotubes (CNTs) and graphene has been proved to be a convenient but effective way for polymer TE property enhancement.[11-17] It should be emphasized that polymer TE materials have unique and intrinsic advantages over inorganic counterparts (such as low cost, convenience to be processed, flexibility and low thermal conductivity (< 1 W $m^{-1}$ $K^{-1}$)). In particular, organic TE materials are promising in certain applications of flexible and portable devices or modules used as off-grid and battery-free power supplies in remote areas or a portable manner, heat removal in electronic devices, *etc.*[6-8,11,12]

Solution-processable free-standing polymer TE films have attracted much of current interests, which can be easily cut into different shapes and various sizes in an exact way, enabling them to suit various conditions.[18-24] Generally, these TE films have been prepared by three methods: vacuum-assisted filtration,[18-20] spin-coating [21,24] and drop-casting.[22,23] The sizes and the thicknesses are normally less than 3.0 cm in diameter and 10–150 μm (thick films) or 100–200 nm (thin films), respectively. Flexible Large-area films for polymer TE materials have seldom been reported. Furthermore, the flexibility of these films was only qualitatively characterized by digital photographs of simply bending. No further quantitative proof and data for flexibility are available so far.

Recently, stretchable electronics have stimulated intense interests in diverse areas such as electronic skins (e-skin),[25,26] stretchable displays,[27] strain/pressure sensors for human motions,[28,29] and energy-related devices.[30,31] Stretchability and mechanical-stability are major intrinsic advantages of organic polymers over inorganic materials. Unfortunately, they have received little attention in TE materials yet. Assuming TE materials were endowed with stretchability and mechanical-stability, they may open widely applications on arbitrary curved and moving surfaces (such as complex machine elements and human joints) to withstand various kinds of mechanical stresses (bending, rolling and twisting, *etc.*). Along this line of consideration, stretchable self-sustainable power sources or devices can be achieved to harvest low-quality or waste heat by polymer TE materials, which can negate the need to periodically replace the power source in complex or extremely environments. However, the studies of stretchability and mechanical-stability in TE materials are very scarce.

Here, we report the first large-area, stretchable, super flexible and mechanically-stable TE films of organic conducting polymer composites. Water-processed, large-area, smooth and

[a] *Institute of Chemistry, Chinese Academy of Sciences, Beijing 100190 (China).E-mail: chengm@iccas.ac.cn*
[b] *School of Chemistry and Chemical Engineering of University of Chinese Academy of Sciences, Beijing 100049 (China).E-mail: cyguo@ucas.ac.cn*
[c] *Sino-Danish Center for Education and Research/Sino-Danish College of University of Chinese Academy of Sciences, Beijing 100190 (China).*

† Footnotes relating to the title and/or authors should appear here.
Electronic Supplementary Information (ESI) available: Digital photographs of PPy/SWCNT composite films and some SEM images. See DOI: 10.1039/x0xx00000x

super flexible polypyrrole/single-walled carbon nanotube (PPy/SWCNT) composites have been prepared by common vacuum filtration method. To study the stretchability, mechanical tensile tests were conducted. The tensile strengths, moduli and elongations at break were measured. Other than direct observations by digital photographs of bending, rolling and twisting, the film super flexibility was further quantitatively investigated by minimum bending radii. In addition, the mechanical stability was investigated by measuring the TE performance after bending and stretching. These features render our composite TE films unique and suitable to a variety of heat energy harvesting applications especially in complex and extremely environments, where various kinds of mechanical stresses need to be endured.

## Experimental

### Materials

Pyrrole (CP, purity ⩾ 98.0 %) and sodium dodecyl sulfate (SDS, AR) were purchased from Sigma Aldrich. SWCNTs (diameter: <3 nm, purity: >85.0 wt%) were provided by Shenzhen Nanotech Port Co. Ltd, China. All of the other reagents, including iron sulfate ($Fe_2(SO_4)_3$) (AR), anhydrous ethanol (AR) and distilled water, were used as received in the preparation procedure without any further purification.

### Preparation of PPy/SWCNT composites

The PPy/SWCNT composites were prepared by an *in situ* chemical oxidative polymerization method with iron sulfate as the oxidant. In a typical synthesis, a desired amount of SWCNT was firstly dispersed in aqueous SDS solution (25 mL, 16 g $L^{-1}$) with or without the presence of ethanol (5 mL) under ultrasonic treatment for 60 min. Then, 50 mg of pyrrole monomer was added into the mixture under ultra-sonication for 10 min. The system was magnetically stirred for 20 min at 0–5 °C. Subsequently, 750 mg of iron sulfate was first dissolved in 4 mL of deionized water and then slowly dropped into the above solution to initiate the polymerization reaction. The reaction occurred at 0–5 °C with constant mechanical stirring for 8 h. After that, the resulting black precipitate was filtered under vacuum and rinsed with ethanol and deionized water for several times until the filtrate became colourless. Finally, flexible and mechanically stretchable PPy/SWCNT composite films were obtained by drying under vacuum at 60 °C for 24 h. The mass ratio of SWCNT to pyrrole monomer varied from 0.1:1 to 0.8:1. For comparisons, the corresponding pure PPy samples were prepared under the same conditions. Note that the pure PPy sample was in the form of powder rather than film.

### Morphological characterization and Raman spectra

The FESEM morphology of the neat PPy or the PPy/SWCNT nanocomposite was observed using HITACHI S-4800 scanning electron microscope. Raman spectra were collected through a Raman spectrometer with an excitation wavelength of 633 nm.

### Mechanical property tests

Mechanical tensile property tests were conducted using an Instron 3365 testing instrument measured at 25 °C. The length, width and thickness for the band-like shape samples were 55 mm, 7 mm and ~0.07 mm, respectively. The distance between the two clamps was 25 mm, and the crosshead speed was 5 mm $min^{-1}$. The quantitative measurements of film flexibility were conducted by rolling the films on cylindrical objects. If the films could be successfully mounted on the objects, their radii were used as the bending radii. The minimum radii were used to characterize the film flexibilities.

### TE performance measurements

The PPy/SWCNT composite films were cut into rectangular shape for electrical conductivity and Seebeck coefficient measurements. The thicknesses of the films were measured by an optical microscope (PDV JX-40). And the pure PPy powder samples were cold pressed at 10 MPa into pellets for TE performance tests. The electrical conductivities were measured by Keithley 2000 Multimeter (Keithley Instruments Inc, USA) using a standard four point configuration method. The Seebeck coefficients were determined by performing a temperature scan at one end of the sample (heating) and measuring the temperature at two points along its length (temperature gradient $\Delta T$). The slope of the linear relationship between the thermoelectromotive force ($\Delta V$) and temperature difference ($\Delta T \approx 10$ K) was then used to obtain the Seebeck coefficient ($S = -\Delta V/\Delta T$).

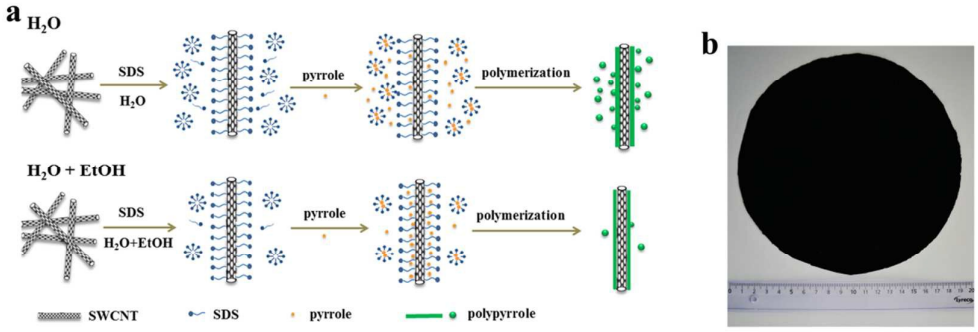


Fig. 1 (a) Schematic illustration showing the preparation procedure for the PPy/SWCNT nanocomposites *via* a template-directed *in situ* polymerization approach with water or aqueous ethanol as reaction medium. (b) A photograph of the PPy/SWCNT nanocomposite thermoelectric film with a diameter of ~18 cm.

## Results and discussion

As shown in Fig. 1a, the PPy/SWCNT nanocomposites were prepared *via* a template-directed *in situ* polymerization approach in aqueous solutions. The effects of medium, water ($H_2O$) or aqueous ethanol ($H_2O$+EtOH), on the preparation, product morphology and properties were compared. First, with the help of sodium dodecyl sulfate (SDS), SWCNTs were dramatically exfoliated and homogeneously dispersed in water or aqueous ethanol. Due to the interfacial attractions of π-π interactions and *van der Waals* forces between SWCNTs and the monomers of pyrrole, most of the pyrrole monomers were adsorbed on the SWCNT surfaces, together with a small amount of pyrrole monomers dissolved in SDS micelles. Subsequently, *in situ* polymerization reaction occurred on the SWCNT surfaces, resulting in a wrapping layer of PPy on SWCNTs. After the composites were washed and filtrated under vacuum, the composite films were achieved.

Fig. 1b shows a typical example of the PPy/SWCNT composite film. A black, smooth and homogeneous film with a diameter of approximately 18 cm can be clearly observed. By judiciously adjusting the amount of Py monomers and SWCNTs as well as the size of the filtration membrane, the composite films with different sizes and thicknesses (20–150 μm) could be conveniently obtained. Compared with the previous publications, the composite films reported herein are of larger area and similar thickness. In addition, the films can be easily cut into a variety of shapes including squares, circles, triangles and stars (Fig. S1† in the Supporting Information).

The wrapping morphology for SWCNT/PPy composite was directly observed by field-emission scanning electron microscopic (FESEM) images. For clarity and brevity, only the images for the composites with SWCNT:Py mass ratio of 20% were shown in Fig. 2a, while other images for those at 10%, 30%, 40%, 60% and 80% mass ratios were presented in Figs. S2† and S3†. Distinctly, unlike the scale-like granular particles for the pure PPy (Fig. S4†), Fig. 2a reveals a quasi-one-dimensional nanostructure for the PPy/SWCNT composite, where PPy layers were tightly enwrapped on the SWCNT surfaces. The average diameters for the composites were around 70 and 60 nm, respectively, much larger than that for the pristine SWCNTs (< 3 nm). Moreover, the small protrusions or lumps on the outer surfaces further confirm the surface coating of polymer layers. Similar coating morphology of conducting polymers on reduced graphene oxide (rGO) or carbon nanotubes (CNTs) have been reported for the TE composites prepared by *in situ* polymerization route.[13-17] In addition, due to the reduction of the PPy relative content, the thickness of the surface coating layers reduced with the increase of SWCNT:Py mass ratios, ranging from 80 nm to 25 nm for the composites prepared in water with the ratios between 10 wt% and 80 wt% (Fig. S2†). In other words, the thickness of the PPy coating layers can be conveniently tuned by adjusting the SWCNT:Py mass ratios.

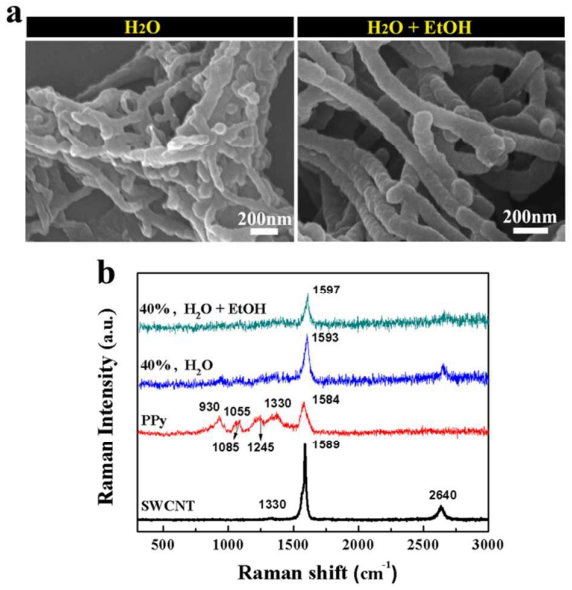


Fig. 2 (a) FESEM images of the composites with SWCNT:Py ratio of 20 wt%, prepared in the medium of water or aqueous ethanol. (b) Raman spectra for the SWCNT, the neat PPy and PPy/SWCNT composites, prepared in water or aqueous ethanol medium.

The effect of reaction medium on the surface coating morphology should be noted. In Fig. S4†, the neat PPy prepared in aqueous ethanol is obviously much more regular in shape and size than that prepared in water, although both are scale-like and granular. The latter looks like irregular agglomerates. As for the composites, Fig. 2a, Figs. S2† and S3† suggest that the outer coating layers for those prepared in aqueous ethanol are distinctly uniform in morphology relative to those prepared in water. Ethanol has been reported to have significant effect on the morphology of neat PPy nanofibres,[32] PPy spherical nanoparticles,[33] PPy/rGO composites[34] and PPy/silica composite[35] *etc.*, by facilitating a more smooth and uniform morphology. It was believed to increase the solubility of Py monomers in water and surfactant micelles,[35] act as co-surfactant to further lower the interfacial energy and optimize the PPy chain structure during interfacial polymerization,[33] increase the rGO dispersion and benefit the diffusion and growth of Py monomers on rGO nanosheet surface.[34]

In order to elucidate the interfacial interaction between SWCNTs and PPy coating layers, Raman spectra were collected. In Fig. 2b, a typical peak for the pristine SWCNT at 1589 $cm^{-1}$ (G-band) is assigned to the $E_{2g}$ mode related to the vibration of $sp^2$-bonded carbon atoms in 2D hexagonal lattices, while the bands at 1330 (D-band) and 2640 $cm^{-1}$ (D'-band) are associated to the disordered feature or defect structures.[36] As for the pure PPy, the bands at 930 and 1085 $cm^{-1}$ are assigned to the quinonoid bipolaronic structure,[37] and the bands at 1055, 1245, 1330 $cm^{-1}$ result from the quinonoid polaronic vibration,[37] anti-symmetrical C-H in-plane bending,[38] and PPy ring stretching mode,[39] respectively. Note that the strong band at 1584 $cm^{-1}$ is attributed to the C=C backbone stretching vibration related to an overlap of two oxidized structures.[38,39] In the Raman spectra of the PPy/SWCNT composites, both bands characteristic of PPy and SWCNTs appear with

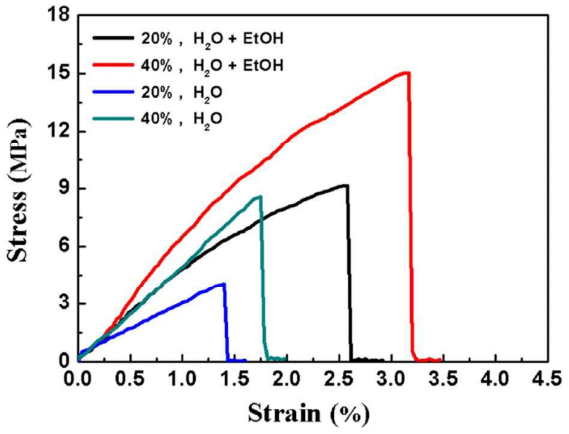


Fig. 3 Stress-strain curves of tensile measurements for the PPy/SWCNT composite films.

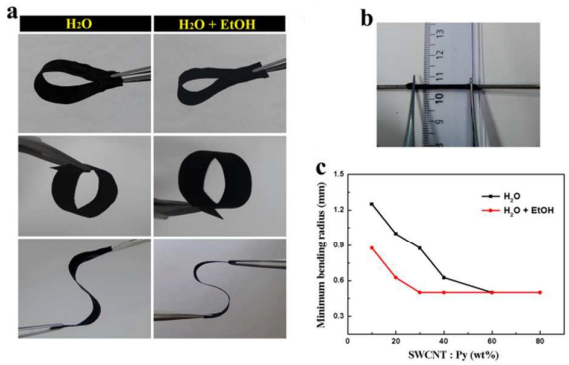


Fig. 4 (a) Digital photographs show that the PPy/SWCNT nanocomposite films exhibited excellent flexibility, and could withstand high levels of deformations by bending, rolling and twisting. (b) Photograph of measurement of minimum bending radius by rolling on a cylindrical object. (c) Minimum bending radii for the composite films with different SWCNT:Py mass ratios, prepared in water or aqueous ethanol medium.

overlapping. Here, the strongest band at 1584 $cm^{-1}$ was employed to study the interfacial interaction. Interestingly, the band shifts distinctly from 1584 $cm^{-1}$ (neat PPy) to 1593 or 1597 $cm^{-1}$ (PPy composites), demonstrating that strong interfacial interactions (π–π conjugated interactions and *van der Waal's* forces) and a charge transfer from PPy to SWCNT took place in the composites.[39] Moreover, the interaction in the composite prepared in aqueous ethanol is more stronger than that prepared in water with a larger band-shift.

Very interestingly, the herein reported PPy/SWCNT composite films revealed important stretchability, in sharp contrast to the lacking of mechanical strength for the neat PPy powder. Although several free-standing TE films of conducting polymers and their composites have been reported,[18–24] we believe that this is the first report of stretchable composite films with TE performance. The mechanical tensile stress-strain curves shown in Fig. 3 reveal that all of the films belonged to brittle fracture without yielding phenomena. Obviously, both SWCNT:Py mass ratios and reaction medium have important effects on mechanical tensile properties. Further detailed data including fracture strengths, tensile moduli and elongations at break were illustrated in Table 1. With the increase of SWCNT:Py ratios, the mechanical properties increased substantially first. The fracture strengths and tensile moduli reached the maxima at 40 wt% and then decreased. On the other hand, the composites prepared in aqueous ethanol revealed greatly increased mechanical properties relative to the corresponding composites prepared in water. For example, when the SWCNT:Py ratio was 40 wt%, the fracture strength, tensile modulus and elongation at break for the composite prepared in aqueous ethanol were 14.2±1.5 MPa, 655±50 MPa and 3.2±0.2%, respectively, much larger than those of the corresponding composite prepared in water (10.0±2.8 MPa, 595±108 MPa and 1.7±0.2%, respectively). The significant increase of mechanical stretchability may result from the strong interfacial interactions (confirmed by Raman spectra) and surface wrapping morphology (shown in FESEM images), which led to effective stress transfer in the composite films. On the other hand, high SWCNT content resulted in possible aggregates and thus deteriorated the mechanical stretchability.

Fig. 4 presents the results of the qualitative and quantitative studies of the flexibility for the PPy/SWCNT composite films. The digital photographs shown in Fig. 4a clearly confirm that the PPy/SWCNT composite films reported herein exhibited excellent flexibility. Rather than flexibility characterization by simple bending in most cases,[18,20-22] the composite films reported herein could withstand high levels of versatile deformations by bending, rolling and twisting without obvious cracking or damage.

**Table 1** Mechanical tensile properties for the PPy/SWCNT composite films.

| SWCNT:Py (wt%) | Fracture strength (MPa) | | Tensile modulus (MPa) | | Elongation at break (%) | |
|---|---|---|---|---|---|---|
| | $H_2O$ | $H_2O$+EtOH | $H_2O$ | $H_2O$+EtOH | $H_2O$ | $H_2O$+EtOH |
| 20 | 5.1±1.9 | 9.5±1.6 | 398±93 | 547±26 | 1.5±0.3 | 2.50.2 |
| 30 | 5.4±0.4 | 14.2±1.1 | 486±62 | 682±112 | 1.5±0.1 | 3.2±0.2 |
| 40 | 10.0±2.8 | 14.2±1.5 | 595±108 | 655±50 | 1.7±0.2 | 3.1±0.3 |
| 60 | 5.8±0.6 | 7.3±1.5 | 353±51 | 418±48 | 2.0±0.3 | 2.6±0.3 |
| 80 | 5.1±1.7 | 8.3±0.6 | 375±99 | 357±49 | 1.7±0.1 | 3.1±0.4 |

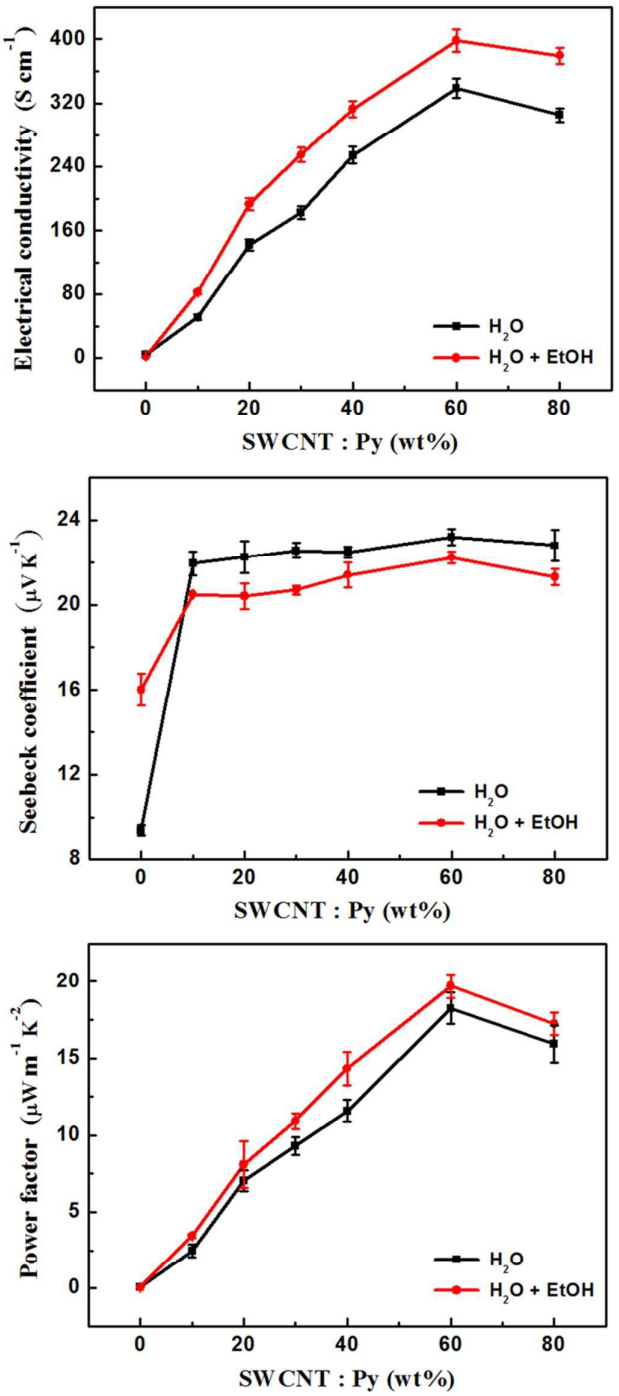


Fig. 5 Electrical conductivities, Seebeck coefficients and power factors at room temperature for the neat PPy and the PPy/SWCNT composite films. The dashed line is the theoretical calculated value based on physical mixing rule.

As mentioned above, no quantitative investigations of film flexibility for polymer TE composites have been reported so far. Here, the super flexibility was quantitatively measured by minimum bending radius *via* rolling on a cylindrical object (Fig. 4b). Very interestingly, the minimum radius for the PPy/SWCNT composite film could reach less than 0.6 mm, confirming the super flexibility.[40] Indeed, the film minimum bending radii were also strongly dependent on SWCNT:Py ratio and reaction medium. They reduced sharply at low SWCNT:Py ratios, and then reached its minimum. On the other hand, aqueous ethanol could increase the flexibility of the composite films, compared with the reaction medium of water.

Fig. 5 shows the electrical conductivities, the Seebeck coefficients and the power factors of the PPy/SWCNT composite films. The neat PPy prepared in water exhibited a low TE performance, with a low electrical conductivity of 4.6±0.1 S cm$^{-1}$, a small Seebeck coefficient of 9.4±0.3 μV K$^{-1}$, and a low power factor of 0.041±0.003 μW m$^{-1}$ K$^{-2}$. The

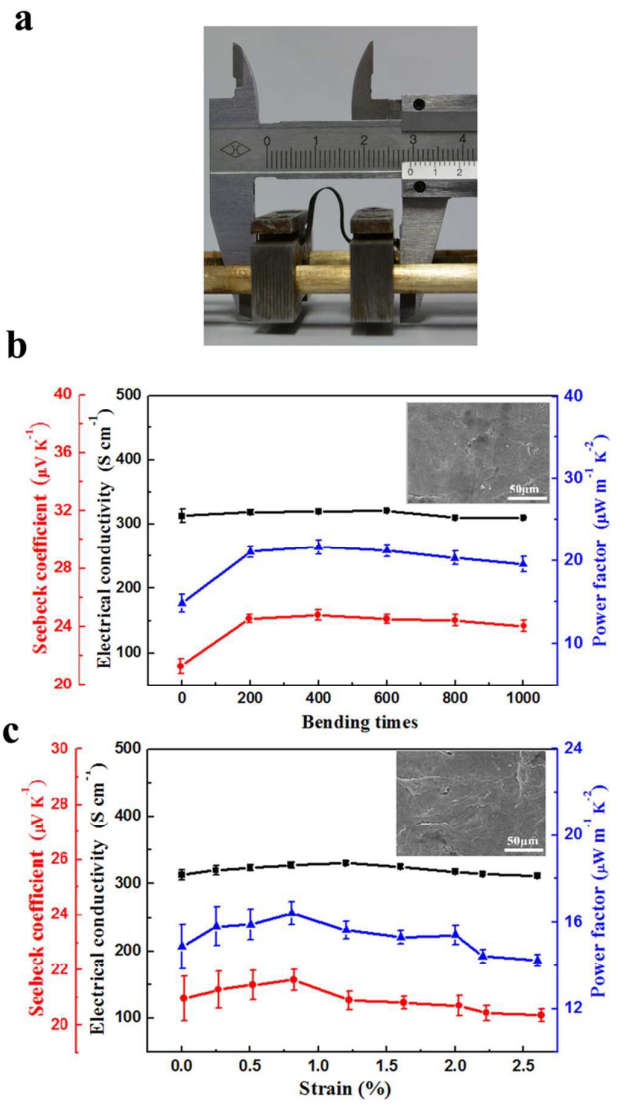


Fig. 6 (a) Bending measurement with a bending radius of 2 mm using a self-made instrument. (b) Thermoelectric performance for the nanocomposite (SWCNT:Py mass ratio of 40 wt%, using aqueous ethanol) before and after bending. (c) Dependence of mechanical stretching on thermoelectric performance for the PPy/SWCNT composite (40 wt%, aqueous ethanol) film. Insets are the FESEM images showing no cracks after (b) bending for 1000 times or (c) stretching to 2.6%.

corresponding TE performance for the PPy prepared in aqueous ethanol were 2.2±0.2 S $cm^{-1}$, 16.0±0.7 μV $K^{-1}$ and 0.06±0.01 μW $m^{-1}$ $K^{-2}$. Importantly, the composite revealed dramatically improved TE performance. Taking the composite with SWCNT:Py ratio of 60 wt% using aqueous ethanol as an example, its electrical conductivity, Seebeck coefficient and power factor reached 399±14 S $cm^{-1}$, 22.2±0.1 μV $K^{-1}$ and 19.7±0.8 μW $m^{-1}$ $K^{-2}$, respectively. Note that the electrical conductivity and the power factor reported herein are the largest values for PPy composites, much higher than the previous maxima of 101.7S $cm^{-1}$ and 10.2 μW $m^{-1}$ $K^{-2}$ for PPy/graphene composite.[41] Moreover, the TE performance showed obvious dependence of SWCNT:Py ratio and reaction medium. The electrical conductivities increased rapidly until the SWCNT:Py ratio of 60 wt% and subsequently decreased, whereas the Seebeck coefficients for the composites were almost independent of the SWCNT:Py ratios. As a whole, the power factors experienced firstly a sharp increase within the SWCNT:Py ratio lower than 60 wt% and a subsequent decrease. On the other hand, the reaction medium had a relatively complex effect on the composite TE performance. The composites prepared in aqueous ethanol had enhanced electrical conductivities but slightly reduced Seebeck coefficients relative to those prepared in water at the same SWCNT:Py ratios. Thus, the TE performances for the composites prepared in aqueous ethanol were higher than those for the corresponding composites prepared in water.

More importantly, the composite films reported herein exhibited excellent mechanical-stable TE performance. Fig. 6a shows the bending measurements with a bending radius of 2 mm by a self-made instrument. As shown in Fig. 6b, after the composite films were bent for as many as 1000 times, all of the electrical conductivities, the Seebeck coefficients and the power factors did not reduce compared with those before bending. Indeed, no obvious changes occurred for the electrical conductivities, while a slightly increase took place for the Seebeck coefficients and the power factors. In the case of stretching, the composite films maintained TE performance very well after being stretched to a strain of 2.6% (Fig. 6c). To elucidate the reason of the excellent mechanical-stable TE performances, FESEM images were collected for the films after being bent for 1000 times and stretched to 2.6%, respectively. Being very similar to the composite film before bending and stretching (Fig. S5†), the inset pictures in Fig. 6b and c clearly demonstrate that no obvious cracks could be observed, confirming the excellent mechanical-stability of TE performance for the present PPy/SWCNT composite films.

## Conclusions

In summary, our work represents a novel insight into polymer TE materials with stretchability, super flexibility and mechanically-stable TE performance, and a remarkable advance toward developing mechanical-stable TE materials for next-generation flexible devices. Both the electrical conductivity and the power factor for the present study are the maximum values for PPy composites. By common vacuum filtration method, large-area TE films with conveniently-tuneable thicknesses and sizes were prepared, which could be easily cut into versatile shapes. Importantly, the mechanical tensile tests strongly confirmed the film stretchability. Very interestingly, the film super flexibility was demonstrated by both direct observations under various deformations (including bending, rolling and twisting) and quantitative measurements of minimum bending radii (< 0.6 mm). Furthermore, we first report the mechanical stability of the TE performance after bending or stretching. In addition, ethanol has important effects on both morphology and properties such as to facilitate the smooth and uninform surface wrapping of PPy on SWCNT, strengthen the interfacial interaction, enhance the mechanical tensile property, flexibility as well as the TE performance (electrical conductivity and power factor ) for the PPy/SWCNT TE composites. It is reasonable to expand the present study of PPy/SWCNT TE composites to other polymers and polymer/inorganic composites. By fully realizing the intrinsic advantages of polymer materials such as stretchability, super flexibility and mechanical stability, these findings reported herein will arouse intense interests of novel energy materials, speed up and widen the applications of organic polymer TE materials.

## Acknowledgements

We thank the National Natural Science Foundation of China (51573190, 51343005) for financial support. G. Chen acknowledges Youth Innovation Promotion Association, Chinese Academy of Sciences.

## Notes and references

1 W. Zhao, P. Wei, Q. Zhang, H. Peng, W. Zhu, D. Tang, J. Yu, H. Zhou, Z. Liu, X. Mu, *Nat. Commun.*, 2015, **6**, 6197.
2 B. Roche, P. Roulleau, T. Jullien, Y. Jompol, I. Farrer, D. A. Ritchie, D. C. Glattli, *Nat. Commun.*, 2015, **6**, 6738.
3 M. Wang, C. Bi, L. Li, S. Long, Q. Liu, H. Lv, N. Lu, P. Sun, Liu M, *Nat. Commun.* 2015, **5**, 4598.
4 D. Yoo, J. Kim, S. H. Lee, W. Cho, H. H. Choi, F. S. Kim, J. H. Kim, *J. Mater. Chem. A* 2015, **3**, 6526.
5 O. Bubnova, Z. U. Khan, A. Malti, S. Braun, M. Fahlman, M. Berggren, X. Crispin. *Nat. Mater.* 2011, **10**, 429.
6 M. He, F. Qiu, Z. Lin, *Energy Environ. Sci.* 2013, **6**, 1352.
7 O. Bubnova, X. Crispin, *Energy Environ. Sci.* 2012, **5**, 9345.
8 Q. Zhang, Y. Sun, W. Xu, D. Zhu, *Adv. Mater.* 2014, **26**, 6829.
9 D. Sheberla, S. Patra, Y. H. Wijsboom, S. Sharma, Y. Sheynin, A. Haj-Yahia, A. H. Barak, O. Gidron, M. Bendikov, *Chem. Sci.* 2015, **6**, 360.
10 X. Hu, G. Chen, X. Wang, H. Wang, *J. Mater. Chem. A* 2015, **3**, 20896.
11 B. T. McGrail, A. Sehirlioglu, E. Pentzer, *Angew. Chem. Int. Ed.* 2015, **54**, 1710.
12 Y. Du, S. Z. Shen, K. Cai, P. S. Casey, *Prog. Polym. Sci.* 2012, **37**, 820.
13 K. Xu, G. Chen, D. Qiu, *J. Mater. Chem. A* 2013, **1**, 12395.
14 Z. Zhang, G. Chen, H. Wang, W. Zhai, *J. Mater. Chem. C* 2015, **3**, 1649.
15 K. Xu, G. Chen, D. Qiu, *Chem. Asian J.* 2015, **10**, 1225.
16 Z. Zhang, G. Chen, H. Wang, X. Li, *Chem. Asian J.* 2015, **10**, 149.

17 S. Han, W. Zhai, G. Chen, X. Wang, *RSC Adv.* 2014, **4**, 29281.
18 D. A. Mengistie, C.-H. Chen, K. M. Boopathi, F. W. Pranoto, L. J. Li, C. W. Chu, *ACS Appl. Mater. & Interfaces*, 2015, **7**, 94.
19 H. Kim, S-G. Park, B. Jung, J. Hwang, W. Kim, *Appl. Phys. A* 2014, **114**, 1201.
20 J. Xiang, L. T. Drzal, *Polymer* 2012, **53**, 4202.
21 N. Massonnet, A. Carella, O. Jaudouin, P. Rannou, G. Laval, C. Celle, J.-P. Simonato, *J. Mater. Chem. C* 2014, **2**, 1278.
22 L. Wang, Q. Yao, H. Bi, F. Huang, Q. Wang, L. Chen, *J. Mater. Chem. A*, 2015, **3**, 7086.
23 F. Kong, C. Liu, H. Song, J. Xu, Y. Huang, H. Zhu, J. Wang, *Synth. Met.* 2013, **31,**185.
24 C. T. Hong, W. Lee, Y. H. Kang, Y. Yoo, J. Ryu, S. Y. Cho, K-S. Jang. *J. Mater. Chem. A*, 2015, **3**, 12314.
25 A. P. Gerratt, H. O. Michaud, S. P. Lacour, *Adv. Funct. Mater.* 2015, **25**, 2287.
26 S. Park, H. Kim, M. Vosgueritchian, S. Cheon, H. Kim, J. H. Koo, T. R. Kim, S. Lee, G. Schwartz, H. Chang, Z. Bao, *Adv. Mater.* 2014, **26**, 7324.
27 T. Sekitani, H. Nakajima, H. Maeda, T. Fukushima, T. Aida, K. Hata, T. Someya, *Nat. Mater.* 2009, **8**, 494.
28 T. Yamada, Y. Hayamizu, Y. Yamamoto, Y. Yomogida, *Nat. Nanotechnol.* 2011, **6**, 296.
29 C. Pang, G. Y. Lee, T. I. Kim, S. M. Kim, H. N. Kim, S. H. Ahn, K. Y. Suh, *Nat. Mater.* 2012, **11**, 795.
30 L. Hu, M. Pasta, F. L. Mantia, L. Cui, S. Jeong, H. D. Deshazer, J. W. Choi, S. Han, Y. Cui, *Nano Lett.* 2010, **10**, 708.
31 G. Tarabella, F. M. Mohammadi, N. Coppedè, F. Barbero, S. Lannotta, C. Santato, F. Cicoira, *Chem. Sci.* 2013, **4**, 1395.
32 X. Zhang, S. K. Manohar, *J. Am. Chem. Soc.* 2004, **126**, 12714.
33 V. M. Ovando-Medina, R. D. Peralta, E. Mendizábal, H. Lara-Ceniceros, T. E. Martínez-Gutiérrez, R. Ledezma-Rodríguez, *Colloid Polym. Sci.* 2011, **289**, 759.
34 J. Zhang, X. S. Zhao, *J. Phys. Chem. C* 2012, **116**, 5420.
35 L. Sun, Y. Shi, L. Chu, Y. Wang, L. Zhang, J. Liu, *J. Appl. Polym. Sci.* 2012, **123**, 3270.
36 F. Inoue, R. A. Ando, C. M. S. Izumi, P. Corio, *J. Phys. Chem. C* 2014, **118**, 18240.
37 S. Demoustier-Champagne, P. Y. Stavaux, *Chem. Mater.* 1999, **11**, 829.
38 T.-M. Wu, H.-L. Chang, Y. W. Lin, *Compos. Sci. Technol.* 2009, **69**, 639.
39 N. G. Sahoo, Y. C. Jung, H. H. So, J. W. Cho, *Synth. Met.* 2007, **157**, 374.
40 H. Kang, S. Jung, S. Jeong, G. Kim, K. Lee, *Nat. Commun.* 2015, **6**, 6503.
41 L. Wang, F. Liu, C. Jin, T. Zhang, Q. Yin, *RSC Adv.* 2014, **4**, 46187.

SYNOPSIS TOC

Large-area, stretchable, super flexible and mechanically-stable thermoelectric films of polymer/carbon nanotube composites